NON-HEME IRON(IV) OXO INTERMEDIATES

A M.Sc. Dissertation report by:

MS. MELISA J. L. DIAS

20P0490017

SCHOOL OF CHEMICAL SCIENCES, GOA UNIVERSITY

April 2022

CERTIFICATE

This is to certify that the dissertation entitled **"Non-heme iron(IV) oxo intermediates"** is bonafide work carried out by Ms. Melisa J. L. Dias under my supervision (Sunder N. Dhuri) in partial fulfillment of the requirement for the award of the degree of Masters of Science in Chemistry at the School of Chemical Sciences, Goa University.

Prof. Dr. Sunder N. Dhuri

(Dissertation Guide)

School of Chemical Sciences

Goa University

Ms. Melisa J. L. Dias

M.Sc. Part-II

Inorganic Chemistry

TABLE OF CONTENT

1. Introduction

Heme and non-heme iron enzymes catalyze a diverse array of important metabolic transformations that require the binding and activation of dioxygen. The catalytic reactions of the enzymes, especially the nature of active oxidizing species, have improved recently with the intensive mechanistic studies of the enzymes and their model compounds.[1] High-valent iron(IV)-oxo intermediates have been identified as reactive species in the catalytic cycles of dioxygen activation by mononuclear non-heme iron enzymes. The intermediates activate substrate C–H bonds to yield hydroxylated, desaturated, or halogenated products.[2],[3] In biomimetic studies, a number of mononuclear non-heme iron(IV)-oxo complexes have been synthesized and characterized by various spectroscopic techniques, and their chemical properties have been investigated in the oxidation of organic substrates and electron-transfer reactions. However, unlike the high-spin (S = 2) iron(IV)-oxo intermediates in non-heme iron enzymes, most of the synthetic non-heme iron(IV)-oxo complexes exhibit a low-spin (S = 1) triplet ground state. Therefore, much effort had been directed towards the synthesis of high-spin iron(IV)-oxo complexes, to understand the effect of the S = 2 ground spin state on the reactivities of non-heme iron(IV)-oxo intermediates in oxidation reactions.[1]

There are three examples of high-spin (S = 2) iron(IV)-oxo complexes reported in biomimetic reactions. The first high-spin iron(IV)-oxo complex, reported by Bakac and co-workers, was synthesized in the reaction of $[Fe^{II}(H_2O)_6]^{2+}$ and ozone in acidic aqueous solution. Very recently, Que and co-workers reported a synthetic high-spin iron(IV)-oxo complex with a trigonal bipyramidal (TBP) geometry, $[(TMG_3tren)Fe^{IV}(O)]^{2+}$ (TMG_3tren = tris(tetramethylguanidino)tren). Subsequently, Borovik and co-workers reported another example of a high-spin iron(IV)-oxo complex with a TBP geometry, $[(H_3buea)Fe^{IV}(O)]^-$ (H_3buea = tris(tert-butylureaylethylene)aminato). Although it had been predicted theoretically that non-heme iron(IV)-oxo species with a ground S = 2 spin state are more reactive than those with an S = 1 iron(IV)-oxo center due to enhancement of exchange stabilization, the high-spin iron(IV)-oxo complex reported by Que and co-workers exhibited a rather sluggish oxidizing power. In a recent computational study, this was shown to originate in steric encumbrance for the access of substrates to the iron-oxo moiety. Thus, it is mandatory to use an iron model without a steric hindrance in gauging reactivities of high-spin iron(IV)-oxo species. In addition, although it had been demonstrated that the reactivity of diiron complexes was dramatically enhanced by converting an S = 1 iron(IV)-oxo center to an S = 2 center, the spin state effect still remains elusive in mononuclear non-heme iron(IV)-oxo models. Mi

Sook Seo and coworkers therefore attempted to synthesize a mononuclear high-spin iron(IV)-oxo complex using a sterically less hindered iron(II) complex with a TBP geometry, to understand the significance of the ground S = 2 spin state of iron(IV)-oxo intermediates in non-heme iron enzymes. Interestingly, the iron(IV)-oxo species synthesized from a TBP iron(II) complex possessed an S = 1 ground spin state instead of an S = 2 spin state. More intriguing was the fact that the S = 1 iron(IV)-oxo complex exhibited a high reactivity capable of activating strong C–H bonds, such as those in cyclohexane (99.3 kcal mol^{-1}), even at a low temperature (e.g., at -40 °C).[1]

Very recently, non-heme iron(IV)–oxo intermediates have been identified as active oxidizing species in the catalytic cycles of *Escherichia coli* taurine:R-ketogultarate dioxygenase (TauD), prolyl-4-hydroxylase, and halogenase CytC3.[4] The intermediates were characterized with various spectroscopic techniques, such as Mössbauer, resonance Raman, and X-ray absorption spectroscopies, showing that the intermediates have a highspin (*S* = 2) iron(IV)–oxo unit with double bond character between the iron ion and oxygen atom. The activation of C–H bonds by the iron(IV)–oxo species was proposed to occur via a hydrogen atom abstraction mechanism (i.e., KIE of ~37). In biomimetic studies, the first indirect evidence for the existence of a mononuclear non-heme iron(IV)–oxo intermediate was reported by Wieghardt and co-workers, but the structure was characterized only with Mössbauer spectroscopy. In 2003, Münck, Nam, Que, and their co-workers reported the isolation of a mononuclear non-heme iron(IV)–oxo complex bearing a macrocyclic ligand. The intermediate has been well-characterized with various spectroscopic techniques and X-ray crystallography, revealing that the intermediate has an iron(IV)–oxo unit with Fe–O double bond character and a low-spin (*S* = 1) Fe(IV) oxidation state. Since then, a number of mononuclear non-heme iron(IV)–oxo complexes bearing tetradentate N4 and pentadentate N5 and N4S ligands have been synthesized and studied in the oxidation of various substrates, such as PPh_3, thioanisoles, *N*,*N*-dialkylanilines, aromatic compounds, alkylaromatic compounds, olefins, alcohols, and alkanes. Thus, the success of generating and isolating mononuclear nonheme iron(IV)–oxo complexes opened a new area in the biomimetic studies of non-heme iron enzymes.[1]

2. First Non-Heme Fe(IV)–Oxo Intermediate

A powerful approach to studying the mechanism of a metalloenzyme-catalyzed reaction is the direct detection of intermediates and their detailed characterization by a combination of

kinetic and spectroscopic methods. Using this approach, one monitors changes in the geometric and/or electronic structure of the metal center during the reaction. This methodology had been used successfully in the 1990s to study O_2 activation by the non-heme diiron proteins methane monooxygenase and the R2 subunit of class I ribonucleotide reductase but was only recently applied to the mononuclear non-heme iron enzymes. The first direct detection of an intermediate in the reaction of a mononuclear non-heme iron enzyme with dioxygen was reported for HPPD. A transient absorption feature at 490 nm that forms with a second-order rate constant of 140 mM^{-1} s^{-1} and decays with a first-order rate constant of 7.8 s^{-1} was noted.[4]

3. Mononuclear Non-Heme Iron(IV)–Oxo Complexes

The first well-characterized mononuclear non-heme iron(IV)–oxo complex was reported in 2003. The late discovery of the non-heme iron–oxo species was due to the difficulty in characterizing non-heme iron(IV)–oxo intermediates by routine spectroscopies like a UV–vis spectrophotometry. The first high-resolution structure of an iron(IV)–oxo species was obtained in non-heme iron models (Figure 1); the success of growing single crystals for X-ray crystallography analysis results from their greater thermal stability. With non-heme iron(IV)–oxo complexes firmly established by crystallography, significant progress has been made in the chemistry of non-heme iron(IV)–oxo intermediates over the past 4 years; ~15 non-heme iron(IV)–oxo complexes appeared in the literature in that time.[1]

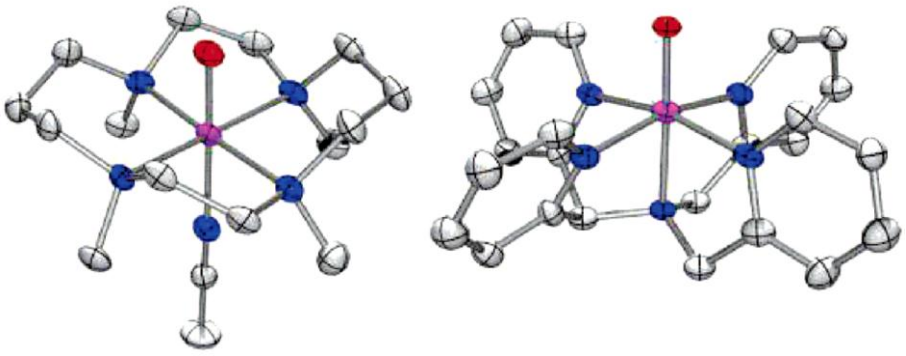

FIGURE 1. X-ray crystal structures of $[Fe^{IV}(TMC)(O)(NCCH_3)]^{2+}$ (left) and $[Fe^{IV}(N4Py)(O)]^{2+}$ (right). Atom colors: gray for carbon, blue for nitrogen, red for oxygen, and purple for iron. This figure is adapted from ref 1 and 3.

4. Generation and Characterization of Non-Heme Iron(IV)–Oxo Complexes

The first direct evidence for the generation of an iron(IV)–oxo intermediate by Wieghardt and co-workers in the reaction of $[Fe^{III}(cyclamacetato)\ (CF_3SO_3)]^+$ and O_3 in acetone and water at –80 °C; the green species was characterized as a low-spin (S = 1) Fe(IV)–oxo intermediate based on Mössbauer analysis.[5] Subsequently, Münck, Nam, Que, and their coworkers reported the first X-ray crystal structure of a mononuclear non-heme iron(IV)–oxo complex that was generated in the reaction of $Fe^{II}(TMC)\ (CF_3SO_3)_2$ and PhIO in CH_3CN at –40 °C (Figure 1). The pale green intermediate, characterized with various spectroscopic methods, such as UV–vis spectroscopy, electrospray ionization mass spectrometry, EPR, Mössbauer, resonance Raman, and magnetic circular dichroism, was assigned as $[(TMC)Fe^{IV}{=}O]^{2+}$ with a low-spin (S = 1) Fe(IV) center and a 1.646 Å Fe–O distance. Since then, a handful of non-heme iron(IV)–oxo complexes have been synthesized using macrocyclic tetradentate N4, tripodal tetradentate N4, and pentadentate N5 and N4S ligands (Figure 2 for ligand structures). The structural analysis of the intermediates by X-ray crystallography for $[(TMC)Fe^{IV}{=}O]^{2+}$ and $[(N4Py)Fe^{IV}{=}O]^{2+}$ (Figure 1) and extended X-ray absorption fine structure (EXAFS) for others revealed a short Fe–O bond distance of ~1.64 Å, indicating double-bond character between the iron ion and the oxygen atom. The Fe–O double-bond character was further supported by ν(Fe–O) frequencies (e.g., ~830 cm^{-1}) of $[Fe^{IV}(TMC)\ (O)\ (X)]^{n+}$ complexes. Mössbauer analysis indicates a low-spin (S = 1) Fe(IV) oxidation state for all of the synthetic non-heme iron(IV)–oxo complexes except $[(H_2O)_5Fe^{IV}{=}O]^{2+}$ which has a high-spin (S = 2) state of Fe(IV) in acidic aqueous media. In enzymes, an iron(IV)–oxo intermediate identified in TauD has a 1.62 Å Fe–O distance and a high-spin (S = 2) Fe(IV) center. Interestingly, low-spin Fe(IV)–oxo complexes exhibit characteristic near-IR absorption bands between 650 and 1050 nm with low extinction coefficients (ε_{max} of 250–400 $M^{-1}\ cm^{-1}$), and it turns out that the IR features serve as a convenient spectral signature in forecasting the formation of low-spin iron(IV)–oxo species.

Various oxygen atom donors were used in generating the iron(IV)–oxo complexes, such as PhIO, peracids (e.g., *m*-CPBA and peracetic acid), $KHSO_5$, and NaOX (X = Cl or Br) as single-oxygen atom donors, hydroperoxides (e.g., H_2O_2 and *tert*-butyl hydroperoxide), and molecular oxygen (Scheme 1).[1] While two-electron oxidation of Fe(II) to the Fe(IV)–oxo species was proposed in the reactions of single-oxygen atom donors (reaction a), Fe(III)–OOR species was homolytically cleaved to form Fe(IV)–O species in the reactions of hydroperoxides (reaction b). In the case of O_2 activation (reaction c), it was found that the

structures of iron(II) complexes and solvents (e.g., alcohols) were important factors in generating iron(IV)–oxo species by activating O_2. A mechanism was proposed in which two molecules of an iron(II) complex react with O_2 to give two molecules of an iron(IV)–oxo species. This mechanism is similar to the O_2 activation by iron(II) porphyrins and relevant to the catalytic cycle of methane monooxygenases (MMOs). In the latter reaction, a dinuclear non-heme iron(II) complex activates O_2 to form a di(μ-oxo)diiron(IV) intermediate that effects the hydroxylation of organic substrates, including CH_4.[5]

The stability of non-heme iron(IV)–oxo complexes is dependent on ligand structures. For example, $[(TMC)Fe^{IV}{=}O]^{2+}$ and $[(N4Py)Fe^{IV}{=}O]^{2+}$ are thermally stable even at room temperature, whereas $[(TPA)Fe^{IV}{=}O]^{2+}$ is stable only at low temperatures (e.g., -40 °C). Also, the stability of iron(IV)–oxo species is markedly dependent on the pH of reaction solutions; $[(N4Py)Fe^{IV}{=}O]^{2+}$ is stable at low pH (i.e., pH 5–6) but decays at a fast rate with an increase in the pH of the reaction solutions. Further, iron–oxo complexes exhibit different reactivities in oxidation reactions, depending on the ligand structures. While $[(TMC)Fe^{IV}{=}O]^{2+}$ oxygenates Ph_3P to Ph_3PO, $[(N4Py)Fe^{IV}{=}O]^{2+}$ shows the capability of oxidizing the C–H bonds of cyclohexane at room temperature. The reactivity of non-heme iron(IV)–oxo complexes is markedly influenced by the axial ligands bound *trans* to the iron–oxo group. As a conclusion, it was demonstrated that the stability and reactivity of non-heme iron(IV)–oxo intermediates were sensitive to the structure of iron complexes, the axial ligand bound to iron ion, and the pH of reaction solutions. With the results, it was possible to investigate the reactivities of nonheme iron(IV)-oxo complexes in a variety of oxidation reactions in detail.[1]

Scheme 1. Generation of Iron(IV)–Oxo Complexes Using Different Oxidants[1]

a) Single oxygen atom donors

$$[(L)Fe^{II}]^{n+} + X\text{-}O \longrightarrow [(L)Fe^{IV}{=}O]^{n+} + X$$

b) Hydroperoxides

$$[(L)Fe^{II}]^{n+} + ROOH \xrightarrow{\text{Oxid.}} [(L)Fe^{III}\text{-}OOR]^{n+} + X \longrightarrow [(L)Fe^{IV}{=}O]^{n+} + RO\bullet$$

c) Molecular oxygen

$$2[(L)Fe^{II}]^{n+} + O_2 \longrightarrow [(L)Fe^{III}\text{-}O\text{-}O\text{-}Fe^{III}(L)]^{2n+} \longrightarrow 2\,[(L)Fe^{IV}{=}O]^{n+}$$

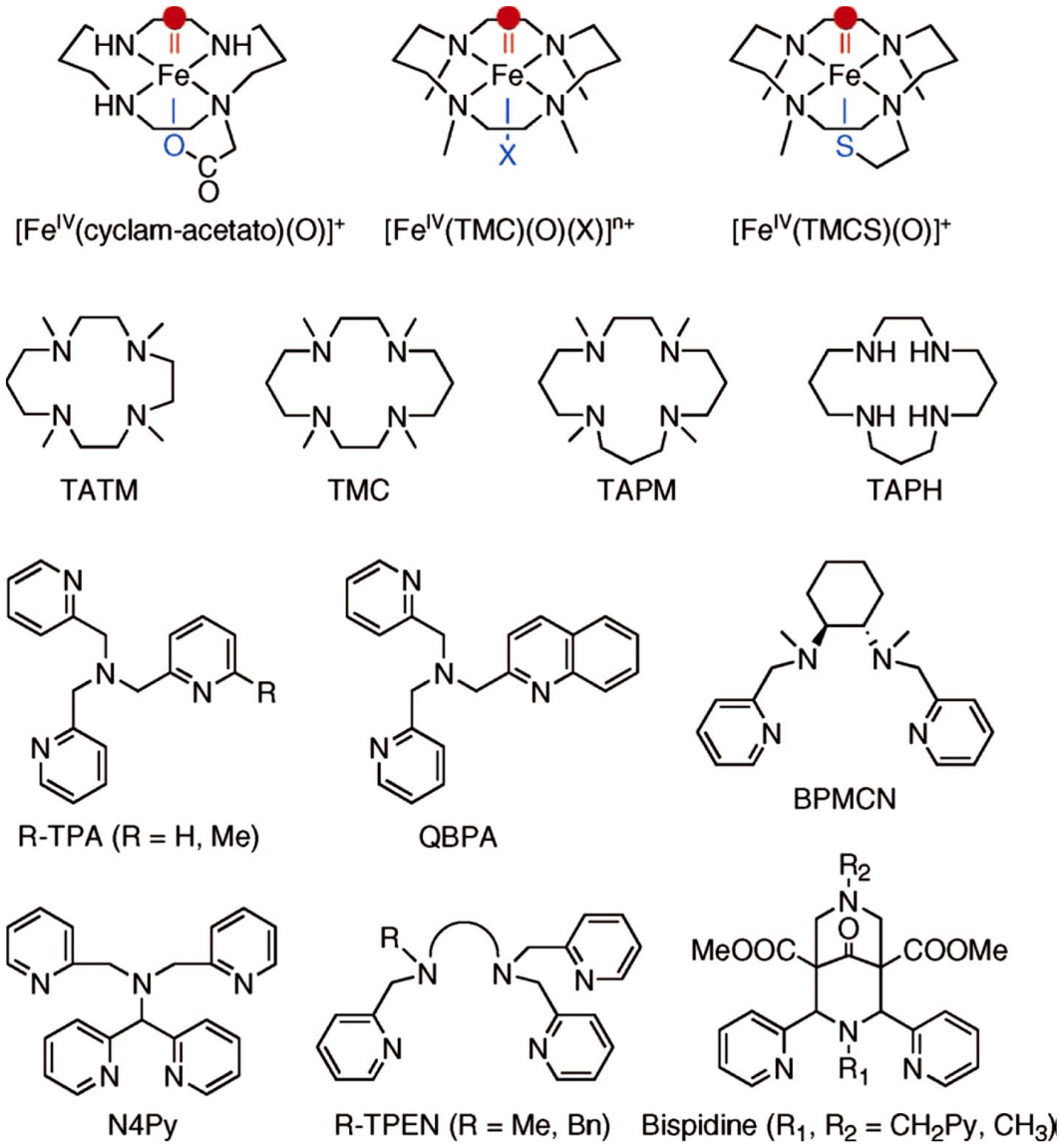

FIGURE 2. Structures of iron(IV)–oxo complexes and ligands. Abbreviations: cyclam-acetate, 1,4,8,11-tetraazacyclotetradecane 1-acetate; TMC, 1,4,8,11-tetramethyl-1,4,8,11-tetraazacyclotetradecane; TMCS, 1-mercaptoethyl-4,8,11-trimethyl-1,4,8,11-tetraazacyclotetradecane; TATM, 1,4,7,10-tetramethyl-1,4,7,10-tetraazacyclotridecane; TAPM, 1,4,8,12-tetramethyl-1,4,8,12-tetraazacyclopentadecane;25 TAPH, 1,4,8,12-tetraazacyclopentadecane; TPA, tris(2-pyridylmethyl)amine; QBPA, (2-quinolylmethyl)bis(2-pyridylmethyl)amine; BPMCN, *N*,*N*-bis(2-pyridylmethyl)-*N*,*N*-dimethyl-*trans*-1,2-diaminocyclohexane; N4Py, *N*,*N*-bis(2-pyridylmethyl)-*N*-bis(2-pyridyl)methylamine; R-TPEN, *N*-R-*N*,*N*′,*N*′-tris(2-pyridylmethyl)ethane-1,2-diamine; Bispidine, 3,7-dimethyl-9,9′-dihydroxy-2,4-di(2-pyridyl)-3,7-diazabicyclononane-1,5-dicarboxylate.

5. Non-Heme Iron(IV)–Oxo Complexes in Oxidation Reactions

The first clear example that non-heme iron(IV)–oxo complexes are capable of transferring their oxygen atom to organic substrates was the oxidation of Ph_3P by $[(TMC)Fe^{IV}{=}O]^{2+}$, yielding Ph_3PO quantitatively (Figure 3, *P*-oxidation). Subsequently, it was demonstrated that an iron(IV)–oxo complex, $[(TPA)Fe^{IV}{=}O]^{2+}$, reacts with cyclooctene to give cyclooctene oxide at –40 °C (Figure 3, alkene epoxidation). Similarly, Girerd and coworkers reported the epoxidation of olefins by $[(Bn\text{-}TPEN)Fe^{IV}{=}O]^{2+}$, in which cyclooctene oxide and *trans*-stilbene oxide were produced in the epoxidation of cyclooctene and *cis*-stilbene, respectively. More recently, Nam and coworkers showed that non-heme iron(IV)–oxo complexes, $[(TPA)Fe^{IV}{=}O]^{2+}$, $[(Bn\text{-}TPEN)Fe^{IV}{=}O]^{2+}$, $[(TPA)Fe^{IV}{=}O]^{2+}$, and $[(TMC)Fe^{IV}{=}O]^{2+}$, are capable of oxygenating sulfides to the corresponding sulfoxides (Figure 3, *S*-oxidation). In the sulfide oxidation, the relative reactivities of the iron–oxo species were in the following order: $[(TPA)Fe^{IV}{=}O]^{2+}$ > $[(Bn\text{-}TPEN)Fe^{IV}{=}O]^{2+}$ > $[(N4Py)Fe^{IV}{=}O]^{2+}$ > $[(TMC)Fe^{IV}{=}O]^{2+}$. The reaction rates were significantly dependent on the electron donating ability of *para* substituents.[1]

The most striking observation made in oxygenation reactions by non-heme iron(IV)–oxo complexes was the hydroxylation of alkanes by $[(N4Py)Fe^{IV}{=}O]^{2+}$ and $[(Bn\text{-}TPEN)Fe^{IV}{=}O]^{2+}$ (Figure 3, aliphatic hydroxylation). The iron(IV)–oxo complexes bearing pentadentate N5 ligands were thermally stable even at room temperature but capable of hydroxylating C–H bonds as strong as those in cyclohexane. More significantly, a large KIE of >30 was observed in the hydroxylation of ethylbenzenes, C_8H_{10} and C_8D_{10}. Such a large KIE implies that the C–H bond activation by non-heme iron(IV)–oxo species occurs via a hydrogen atom abstraction mechanism (Scheme 2). In non-heme iron enzymes, large isotope effects were observed in H-atom abstraction reactions by the iron(IV) intermediates of the monoiron TauD (i.e., KIE of ~37) and the diiron MMO (i.e., KIE of >50).[6]

A large KIE of ~50 was also observed in the oxidation of benzyl alcohol by non-heme iron(IV)–oxo complexes, $[(TPA)Fe^{IV}{=}O]^{2+}$ and $[(N4Py)Fe^{IV}{=}O]^{2+}$ (Figure 3, alcohol oxidation). Such a large KIE value indicates that non-heme iron(IV)–oxo intermediates activate alcohols exclusively by H-atom abstraction from the R-CH group of benzyl alcohol (Scheme 3, pathway A) and that C–H bond cleavage is the rate-determining step. The mechanism of the alcohol oxidation was further investigated with an ^{18}O-labeled iron(IV)–oxo complex, $[(N4Py)Fe^{IV}{=}{}^{18}O]^{2+}$, to understand whether the final step of the alcohol

oxidation occurs via a *gem*-diol dehydration or a dual-hydrogen abstraction process. The product formed in the ^{18}O-labeled experiment contained only a trace amount of ^{18}O, supporting the possibility that the alcohol oxidation by non-heme iron(IV)–oxo complexes occurs via a dual-hydrogen abstraction mechanism (Scheme 3, pathway C), not via a *gem*-diol dehydration process **(**Scheme 3, pathway B).[1]

In contrast to the alkane hydroxylation and alcohol oxidation, Nam and coworkers obtained a low KIE value of ~0.9 in the hydroxylation of aromatic compounds by non-heme iron(IV)–oxo complexes (Figure 3, aromatic hydroxylation).In the hydroxylation of anthracene by [(N4Py)Fe^{IV}═O]$^{2+}$ and [(Bn-TPEN)Fe^{IV}═O]$^{2+}$, anthraquinone was produced in high yields.

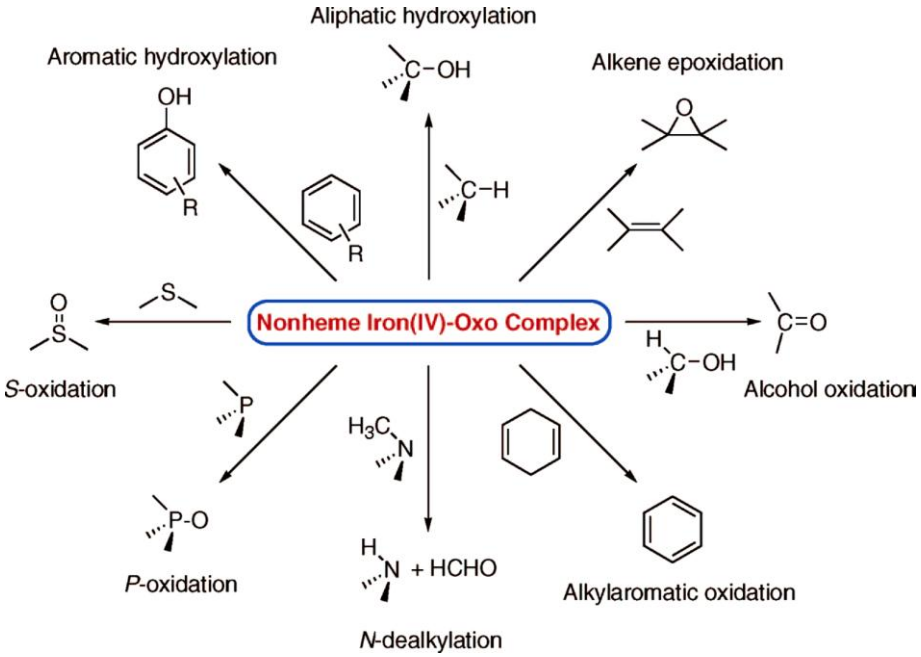

FIGURE 3. Oxidation reactions mediated by mononuclear non-heme iron(IV)–oxo complexes.

Nam and coworkers also found that the electron donating ability of *para* substituents on anthracene influenced reaction rates significantly, affording a large Hammett ρ value of –3.9. Such a large negative ρ value implied that the iron–oxo group attacked the aromatic ring via an electrophilic pathway. Further, the calculated k_H/k_D values of ~0.9, determined kinetically in the hydroxylation of anthracene and deuterated anthracene, indicated an inverse KIE in the aromatic ring oxidation reactions; the observation of the inverse KIE was consistent with the sp^2-to-sp^3 hybridization change during the addition of an electrophilic iron–oxo group to the

sp^2 center of the aromatic ring to form a σ adduct. On the basis of the large negative Hammett ρ and inverse KIE values, they proposed that the aromatic ring oxidation does not occur via a hydrogen atom abstraction mechanism but involves an initial electrophilic attack on the π-system of the aromatic ring to produce a tetrahedral radical or cationic σ complex.[7]

Non-heme iron enzymes participate in oxidative N-dealkylation reactions in nature, and high-valent iron(IV)–oxo species have been invoked as an active oxidant that effects the oxygenation of organic substrates. Nam and coworkers therefore performed oxidative N-dealkylation of *N*,*N*-dialkylamines with non-heme iron(IV)–oxo complexes. In the oxidative N-dealkylation of *N*,*N*-dimethylaniline by $[(N4Py)Fe^{IV}{=}O]^{2+}$ and $[(TMC)Fe^{IV}{=}O]^{2+}$, *N*-methylaniline was produced as a major product with the concurrent formation of CH_2O. Detailed mechanistic studies were carried out in an effort to understand whether the oxidative N-dealkylation occurs via an electron transfer–proton transfer (ET–PT) mechanism or a hydrogen atom transfer (HAT) (Scheme 4). On the basis of the results of a linear free energy correlation (e.g., Hammett ρ values of approximately –2.5), inter- and intramolecular kinetic isotope effects (e.g., KIE values of <5), and product analysis with mechanistic probes, the oxidative N-dealkylation reactions by non-heme iron(IV)–oxo complexes were proposed to occur via an ET–PT mechanism (Scheme 4).[8]

Scheme 2. Alkane Hydroxylation by an Iron(IV)–Oxo Complex

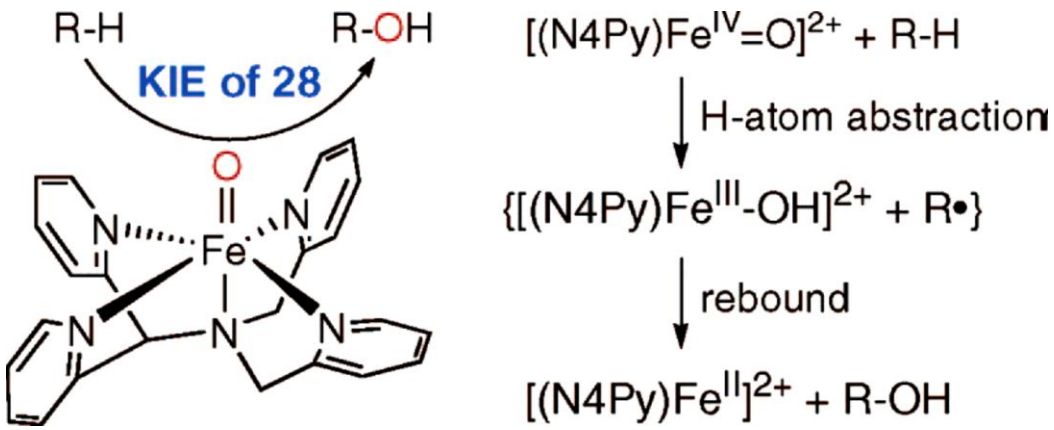

Scheme 3. Proposed Mechanism for Alcohol Oxidation by Iron(IV)–Oxo Species

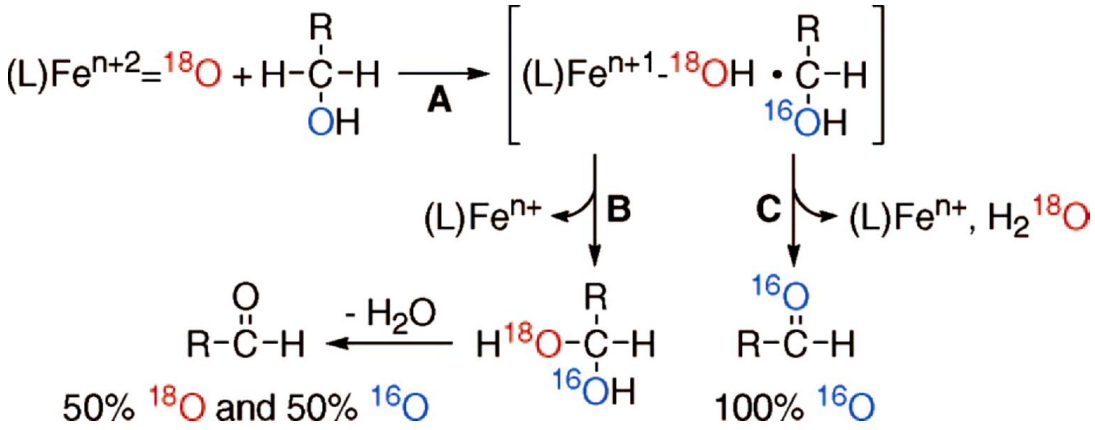

Scheme 4. Proposed Mechanisms for Oxidative N-Demethylation by Fe(IV)–Oxo Complexes

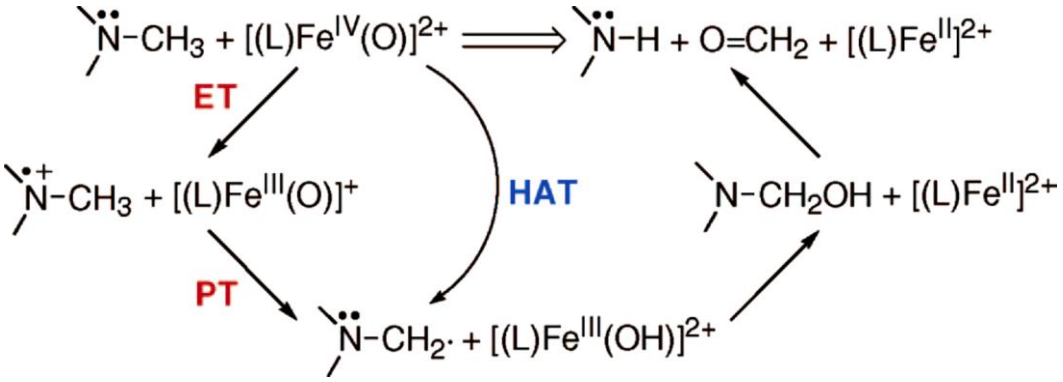

6. Non-heme Iron Oxo Intermediates in Biology

Non-heme proteins activate dioxygen or hydrogen peroxide to generate high-valent oxo iron reactive intermediates, which are used to carry out a diverse set of biological tasks. Important processes such as catabolism, angiogenesis, respiration, and apoptosis rely on oxidation reactions driven by these reactive intermediates. The coordination environment of the oxo iron unit is, however, found to be different in different enzymes. High valent iron–oxo active sites have been identified in non-heme enzymes. This involves mononuclear iron centres that are coordinated to two histidines and a carboxylate group, thereby forming a characteristic 2-His-1-carboxylate facial triad, which has been recognized as a common structural motif for many mononuclear non-heme iron enzymes. Most of these enzymes activate dioxygen in the

iron(II) state and carry out a variety of two-electron oxidation processes; the remaining two reducing equivalents required for the four-electron reduction of dioxygen are often provided by a cosubstrate. One specific group of non-heme enzymes utilizes 2-oxoacids or tetrahydrobiopterin as the cosubstrate, delivering two electrons simultaneously to the active site to afford peroxoiron(II) and oxoiron(IV) species. [9]

These high-valent iron–oxo intermediates in biology have been primarily characterized by ^{57}Fe Mössbauer spectroscopy, as it serves as a local probe of the iron centre. Mössbauer isomer shift (δ) are directly related to the electron density at the iron nucleus and, therefore, are often used as a probe of the 'oxidation state' of the metal. The quadrupole splitting (ΔE_Q) values, on the other hand, are a measure of the electric field gradient at the iron nucleus and can be strongly correlated to electronic spin ground state and molecular geometry. Nuclear hyperfine tensors (A) depend strongly on the nature of the orbitals in which unpaired electrons reside and may be used as a tool to understand the electronic structure of paramagnetic species. Whereas δ and ΔE_Q values obtained from zero-field Mössbauer studies of the active oxidants in non-heme oxygenases are consistent with an iron(IV) oxidation state. In non-heme, a high-spin S = 2 state is demonstrated by 'three large negative' A tensors. The high-spin configuration is possibly due to the weak ligand field exerted by the combination of histidine and carboxylate ligands or the proposed pseudo-trigonal symmetry, which renders the d($x^2 - y^2$) and d(xy) orbitals nearly degenerate in energy.[10]

7. Conclusion

Non-heme iron-oxo complexes were elusive intermediates implicated as powerful oxidants in a variety of important biochemical transformations. Within this context, 2003 marked a year of breakthroughs with contemporaneous reports of the trapping and spectroscopic characterization of the first Fe^{IV}═O intermediate of a nonheme iron enzyme by Bollinger and Krebs and of the synthesis and crystal structure of the first synthetic nonheme Fe^{IV}═O complex by Münck, Nam and Que. Since these groundbreaking discoveries, a wealth of synthetic, structural, and spectroscopic data has been accumulated to provide us with detailed insights into the structure and function of the active oxidants found in nonheme iron enzymes.

All synthetic nonheme Fe^{IV}═O complexes display unique low intensity NIR electronic absorption features, providing a convenient spectroscopic probe for facile identification. The Fe^{IV}═O unit has an Fe–O bond distance ~1.64 Å, as characterized by XRD and/or XAS, and υ_{Fe-O} value of 830 cm^{-1}, observed either by FT-IR or resonance Raman spectroscopy. Mössbauer spectroscopy provides key insights into the electronic structure of the iron center, including oxidation and spin states, and has proven to be the central tool in the analysis of Fe^{IV}═O complexes. More recently, parallel mode EPR has been shown to be an alternative technique to Mössbauer spectroscopy for identifying S = 2 Fe^{IV}═O complexes. Computational studies utilizing density functional theory techniques have also been quite helpful in shedding light on this area of investigation. In the context of the reactivity of Fe^{IV}═O complexes toward C-H bonds, the S = 2 state would thus be predicted to be more reactive than its S = 1 counterpart.

The reactivities and mechanisms of non-heme iron(IV)–oxo complexes in oxygenation reactions over the past 7 years have been reviewed. Non-heme iron(IV)–oxo studies were initiated with the success of obtaining the first crystal structure of a mononuclear non-heme iron(IV)–oxo complex with the groups of Que and Münck. Despite a short history of non-heme iron(IV)–oxo species, significant developments were made in characterizing the intermediates and understanding their reactivities in a variety of oxygenation reactions. The reactions depicted in Figure 2 clearly demonstrate that mononuclear non-heme iron(IV)–oxo complexes are involved in diverse oxygenation reactions. The next challenging target in biomimetic studies of non-heme iron enzymes is to understand the reactivities of the recently discovered non-heme iron(V)–oxo intermediate.

8. Bibliography

[1] W. Nam, "High-valent iron(IV)-oxo complexes of heme and non-heme ligands in oxygenation reactions," in *Accounts of Chemical Research*, Jul. 2007, vol. 40, no. 7, pp. 522–531. doi: 10.1021/ar700027f.

[2] M. S. Seo *et al.*, "A mononuclear nonheme iron(IV)-oxo complex which is more reactive than cytochrome P450 model compound I," *Chemical Science*, vol. 2, no. 6, pp. 1039–1045, Jun. 2011, doi: 10.1039/c1sc00062d.

[3] C. He and Y. Mishina, "Modeling non-heme iron proteins," *Current Opinion in Chemical Biology*, vol. 8, no. 2. pp. 201–208, Apr. 2004. doi: 10.1016/j.cbpa.2004.02.002.

[4] C. Krebs, D. G. Fujimori, C. T. Walsh, and J. M. Bollinger, “Non-heme Fe(IV)-oxo intermediates,” in *Accounts of Chemical Research*, Jul. 2007, vol. 40, no. 7, pp. 484–492. doi: 10.1021/ar700066p.

[5] A. R. McDonald and L. Que, “High-valent nonheme iron-oxo complexes: Synthesis, structure, and spectroscopy,” *Coordination Chemistry Reviews*, vol. 257, no. 2. pp. 414–428, Jan. 05, 2013. doi: 10.1016/j.ccr.2012.08.002.

[6] C. v Sastri *et al.*, “Axial ligand tuning of a nonheme iron(IV)-oxo unit for hydrogen atom abstraction,” 2007. [Online]. Available: www.pnas.org/cgi/content/full/

[7] V. Larson, B. Battistella, K. Ray, N. Lehnert, and W. Nam, “HIGH-VALENT METAL-OXO SPECIES: Iron and Manganese Oxo Complexes, Oxo Wall and Beyond.”

[8] C. Winslow, H. B. Lee, M. J. Field, S. J. Teat, and J. Rittle, “Structure and Reactivity of a High-Spin, Nonheme Iron(III)-Superoxo Complex Supported by Phosphinimide Ligands,” *J Am Chem Soc*, vol. 143, no. 34, pp. 13686–13693, Sep. 2021, doi: 10.1021/jacs.1c05276.

[9] U. K. Bagha *et al.*, “ Oxidative dehalogenation of halophenols by high-valent nonheme iron(iv)-oxo intermediates ,” *Faraday Discussions*, 2022, doi: 10.1039/d1fd00064k.

[10] J. Hohenberger, K. Ray, and K. Meyer, “The biology and chemistry of high-valent iron-oxo and iron-nitrido complexes,” *Nature Communications*, vol. 3. Nature Publishing Group, 2012. doi: 10.1038/ncomms1718.